Supplementary Information

The Effect on Photochemical Smog of Converting the U.S. Fleet of Gasoline Vehicles to Modern Diesel Vehicles

[1]Mark Z. Jacobson, [2]John H. Seinfeld, [3]Greg R. Carmichael, [4]David G. Streets

[1]Department of Civil and Environmental Engineering, Stanford University, Stanford, California 94305-4020, USA. Email: jacobson@stanford.edu

[2]Departments of Chemical Engineering and Environmental Science and Engineering, California Institute of Technology, Pasadena, California, 91125, USA. Email: seinfeld@caltech.edu

[3]Department of Chemical and Biochemical Engineering, University of Iowa, Iowa City, Iowa, 52242-1219, USA; Email gcarmich@icaen.uiowa.edu

[4]Argonne National Laboratory, Argonne, Illinois, 60439, USA. Email: dstreets@anl.gov

Geophysical Research Letters, Paper 2003GL018448, 2003

Introduction

This Supplementary Information describes the model used for this study in more detail, shows paired-in-time-and-space comparisons of model predictions with data for the August baseline case, shows additional difference plots resulting from the switch from gasoline to diesel, and briefly discusses the issue of diesel versus gasoline effects on climate.

1. Description of the model.

GATOR-GCMOM is a nested, parallelized, and vectorized global-through-urban scale air pollution/weather forecast/climate model. The model has been compared with paired-in-time-and-space gas, aerosol, radiative, and meteorological data from the SCAQS field campaign, paired-in-time-and-space gas, radiative, and meteorological data from the SARMAP field campaign, and global data and climatologies [*Jacobson et al.*, 1996; *Jacobson*, 1997, 2001a,b, 2002a]. Here, the model treated time-dependent gas, aerosol, radiative, dynamical, cloud, land-surface, soil, and ocean processes over two layers of nesting, where a 0.5^{o}S-N x 0.75^{o}W-E (about 55 km S-N x 68 km W-E) regional U.S. grid was nested within a 4^{o}S-N x 5^{o}W-E global grid. The global grid included 39 sigma-pressure layers from the ground to 0.425 mb (≈55 km), including 23 tropospheric layers and 4 layers below 1.3 km. The regional grid included 26 layers from the ground to 103.5 mb. The nesting time interval for passing meteorological and chemical variables was one hour.

Gas processes solved in both nested grids included emissions, chemistry (90 species and 205 reactions), gas-aerosol-surface chemistry, advection, turbulence, cloud convection, aerosol nucleation, condensational growth, dissolutional growth, dry deposition, dissolution into cloud and precipitation liquid, and interaction with radiation. Size- and composition-resolved aerosol processes solved included emissions, homogeneous nucleation, coagulation, condensation, dissolution, water uptake by hydration, liquid- and solid-phase equilibrium chemistry, irreversible aqueous chemistry, advection, turbulence, cloud convection, dry deposition, settling, rainout, washout, and interaction with radiation. The most recent description of aerosol processes is described in Jacobson (2002b). Cloud microphysics and interactions with gases and aerosols are

described in Jacobson (2003). Radiation processes included solar and infrared interactions with gases, size- and composition-resolved aerosol particles, and size- and composition-resolved hydrometeor particles. Radiation calculations affected photolysis and heating rates. The dynamical/ocean modules solved for winds, temperatures, pressures, turbulence, sea-surface temperatures, ocean velocities, ocean mixed-layer depth, soil, road, and roof temperatures, and soil moisture.

Meteorological fields, predicted in the model, were initialized for both nested grids on February 1 and August 1, 12 GMT with reanalysis fields from the *National Center for Environmental Prediction* [2003]. Aerosol and gas fields in both domains were first initialized as described in *Jacobson* [2001a,b] Such initial fields were then overridden over the U.S. for O_3, CO, NO_2, SO_2, $PM_{2.5}$, and PM_{10} using U.S. EPA ambient air quality data [*USEPA*, 2003a], interpolated from over 1650 stations to model grid cell at the time corresponding to initialization.

The U.S. EPA emission inventory used [*USEPA*, 2003b] was the 1999 National Emission Inventory, Version 2. Emissions from each source and location were allocated temporarily (with one-hour resolution) and by species with USEPA temporal and speciation factors (NO_x was fractionated into NO and NO_2, TOGs were fractionated into methane, paraffins, ethane, other olefins, formaldehyde, other aldehydes, toluene, xylene, and isoprene; SO_x was fractionated into SO_2 and SO_3, and $PM_{2.5}$ and PM_{10} were fractionated into organic matter, black carbon, sulfate, nitrate, and other).

Biogenic emissions of biogenic isoprene, monoterpenes, other VOCs, and NO for North America were derived from 1-km vegetation and land-use data from the third generation Biogenic Emissions Landuse Database (BELD3) [*USEPA*, 2003c] and for the rest of the world from USGS 1-km landuse/landcover data [*USGS*, 1999]. A program was written to produce normalized (at a specific temperature and radiation level) inventories of biogenic isoprene, monoterpenes, other VOCs, and NO from these data for any spatial and temporal grid. These normalized data were combined in the model with temperature- and radiation-dependent equations to derive emission rates affected by the current temperature and radiation fields.

Emissions of anthropogenic black carbon (BC) and organic matter outside the U.S. were obtained from *Bond et al*. [2003] and for within the U.S., from *USEPA* [2003b]. Emissions of biomass burning, sea spray, soil dust, lightning NO, ocean DMS, volcanic SO_x, and other global sources of NO_x, SO_x, NH_3, CH_4, CO, N_2O, organics, and CO_2 are described in *Jacobson* [2001b].

2. Paired-in-time-and-space comparisons of model with data.

The figures below compare paired-in-time-and-space modeled with measured variables from the August 1999 baseline simulation described in the main paper. The time resolution of the data (and model values) was 1 hour in all cases. Modeled values were interpolated with bilinear interpolation from four surrounding grid cells to the exact location of the measurement. There was no data assimilation (nudging) of any parameter or spinup of the simulations.

Figures 1-8 compare modeled near-surface ozone, near-surface nitrogen dioxide, near-surface isoprene, surface air pressure, near-surface relative humidity, surface solar radiation, surface ultraviolet radiation, and near-surface temperature, respectively, with hourly U.S. air quality data at several sites. All comparisons are paired-in-time-and-space. Although the model captured diurnal variations and several daily peaks of O_3 very well, nighttime O_3 titration by NO_x was often incomplete, possibly due in part to the coarser resolution of the regional grid (0.5^ox0.75^o) relative to the scale over which local O_3 destruction by titration occurs ($<0.05^o$). It may also have been due to slightly

excessive modeled vertical downmixing of O_3 at night. Several nighttime O_3 reductions were simulated correctly.

Figure 1. Comparison of August 1999 hourly modeled (solid lines) with measured (dashed lines) near-surface O_3 [*USEPA*, 2003a] at six air quality monitoring stations in the U.S. Station locations are shown in Figure 2a of the main paper. The simulations were run without data assimilation or spinup. Model results were interpolated with bilinear interpolation from four surrounding grid cells of resolution 0.5°S-N x 0.75°W-E to the location of interest.

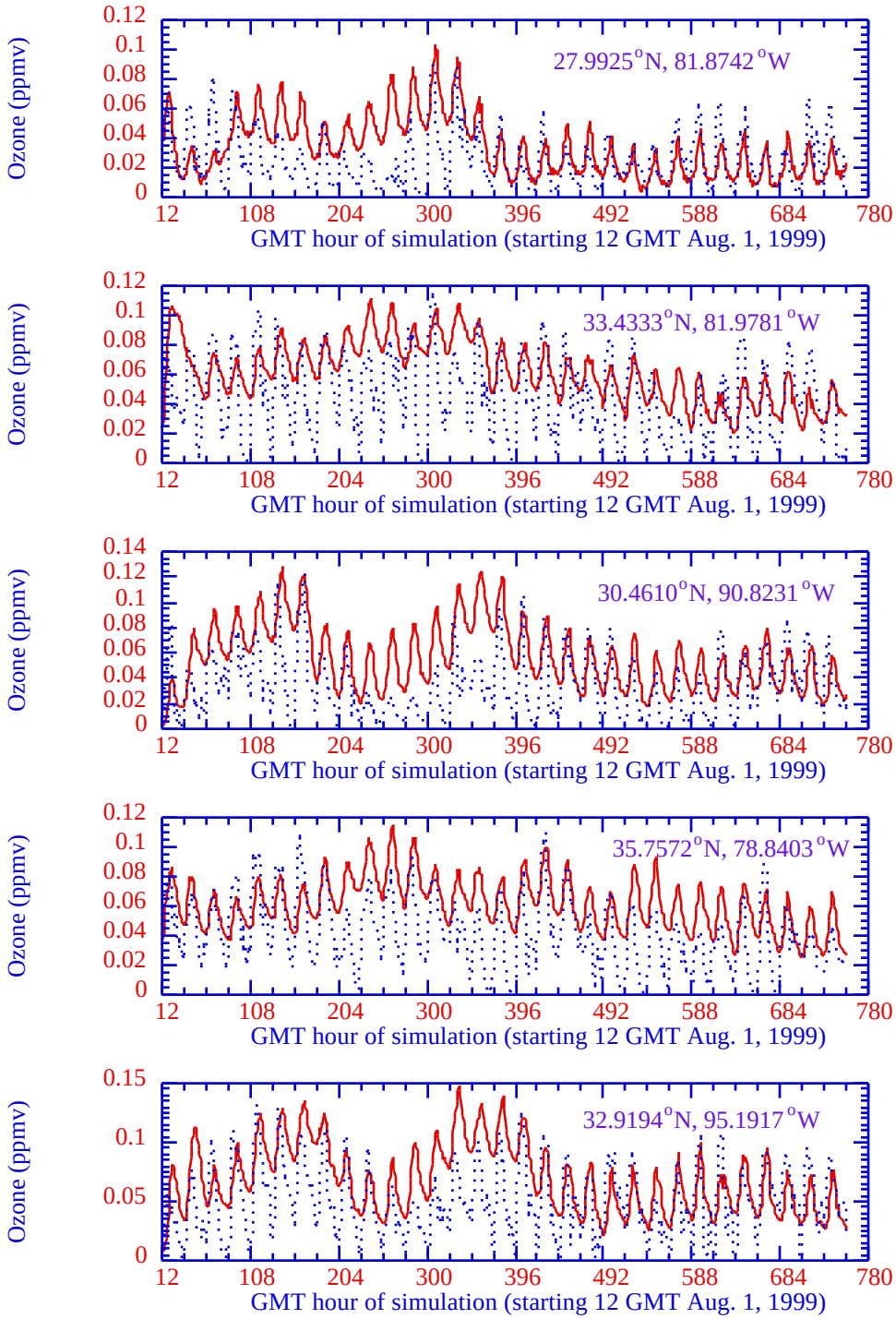

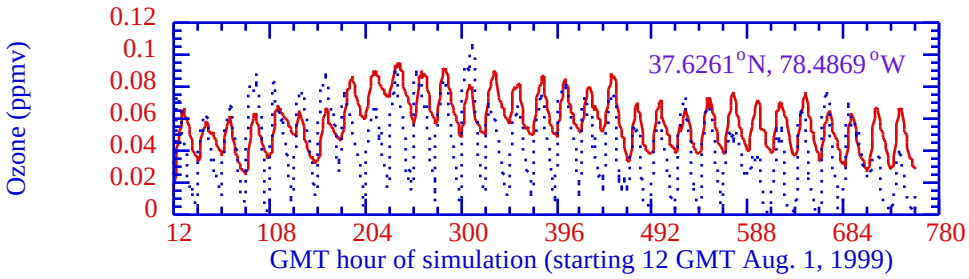

Figure 2a. August 1999 monthly-average modeled baseline near-surface nitrogen dioxide mixing ratio. The red dots represent locations of model comparisons with data in Figure 2b.

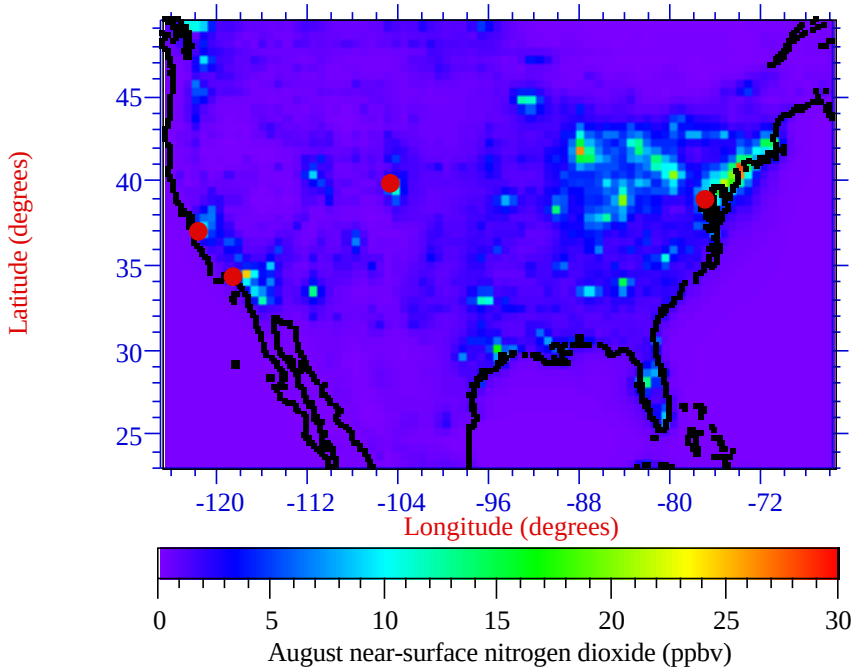

Figure 2b. Comparison of August 1999 hourly modeled (solid lines) with measured (dashed lines) near-surface NO_2 [*USEPA*, 2003a] at four air quality monitoring stations in the U.S. Station locations are shown in Figure 2a. See caption to Figure 1 for resolution of simulation.

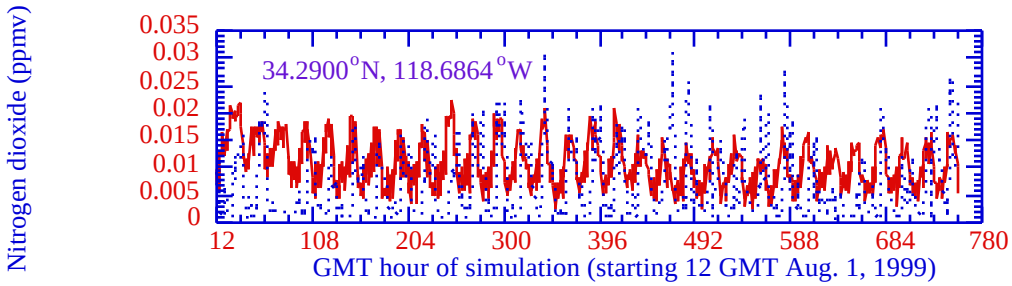

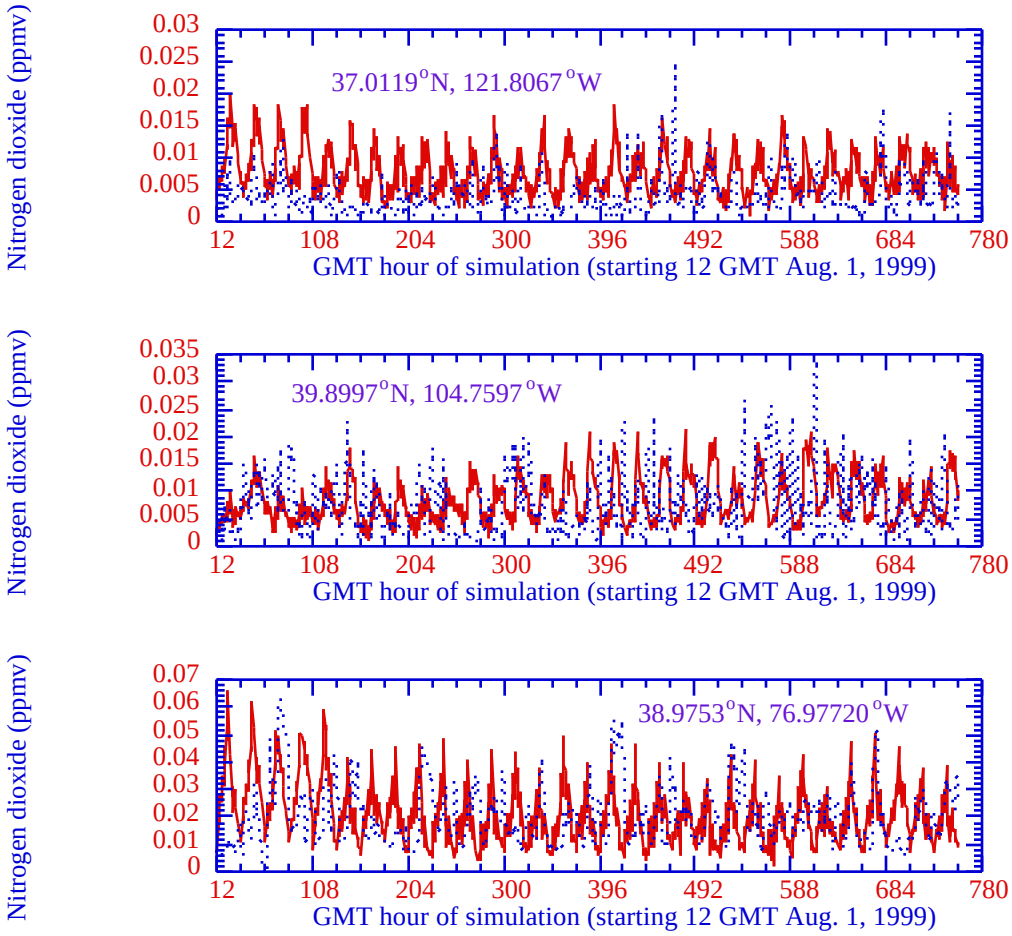

Figure 3a. August monthly-average modeled baseline isoprene mixing ratio. The red dots represent locations of model comparisons with data in Figure 3b.

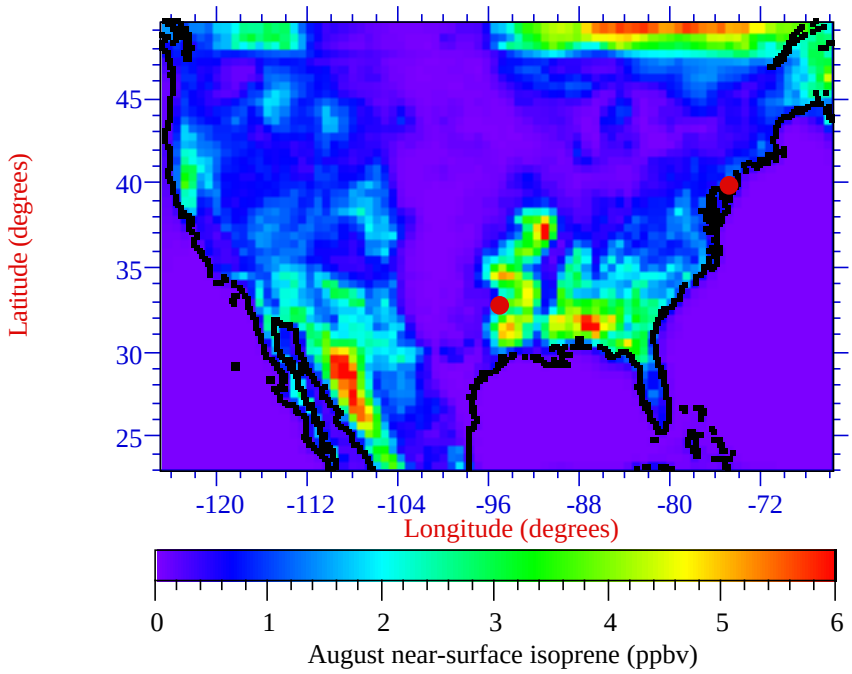

Figure 3b. Comparison of August 1999 hourly modeled (solid lines) with measured (dashed lines) near-surface isoprene [*USEPA*, 2003a] at two air quality monitoring stations in the U.S. Station locations are shown in Figure 2c of the main paper, which shows the baseline August monthly-averaged map of modeled isoprene. See caption to Figure 1 for resolution of simulation.

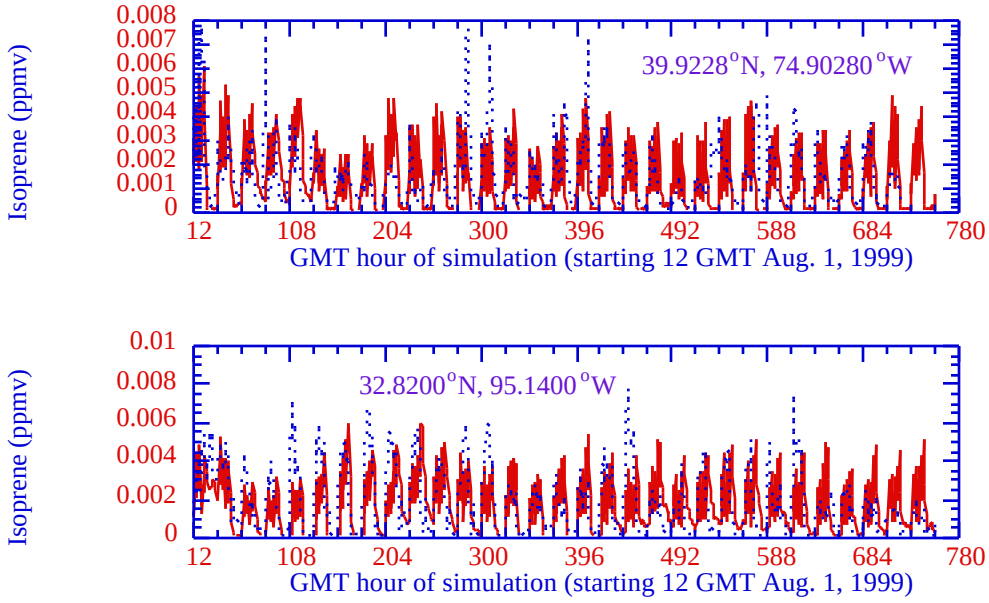

Figure 4. Comparison of August 1999 hourly modeled (solid lines) with measured (dashed lines) surface air pressure [*USEPA*, 2003a] at several air quality monitoring stations in the U.S. See caption to Figure 1 for resolution of simulation.

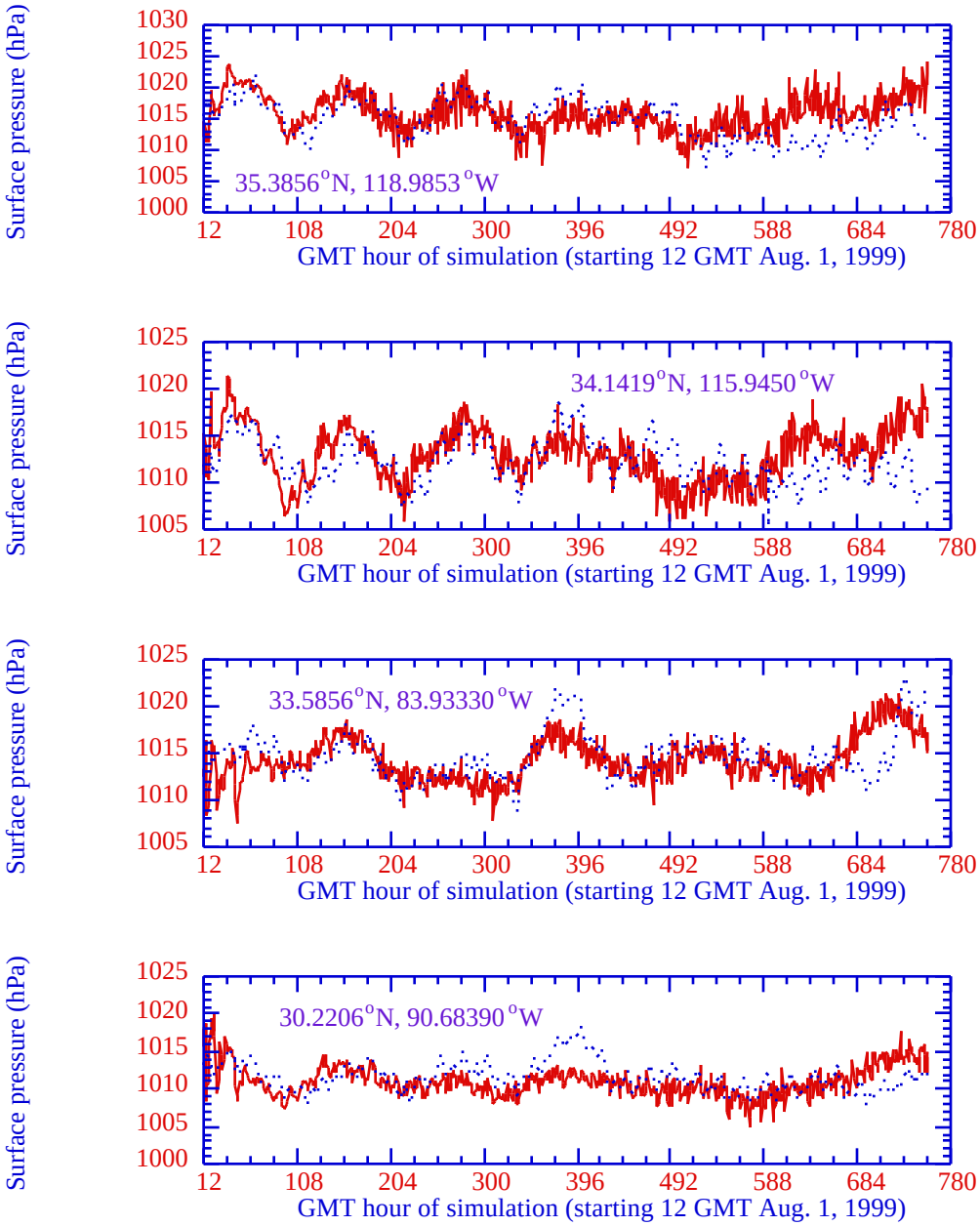

Figure 5. Comparison of August 1999 hourly modeled (solid lines) with measured (dashed lines) near-surface relative humidity [*USEPA*, 2003a] at several air quality monitoring stations in the U.S. See caption to Figure 1 for resolution of simulation.

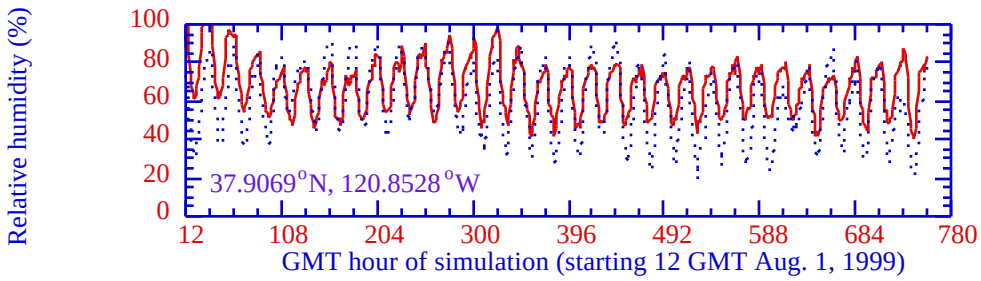

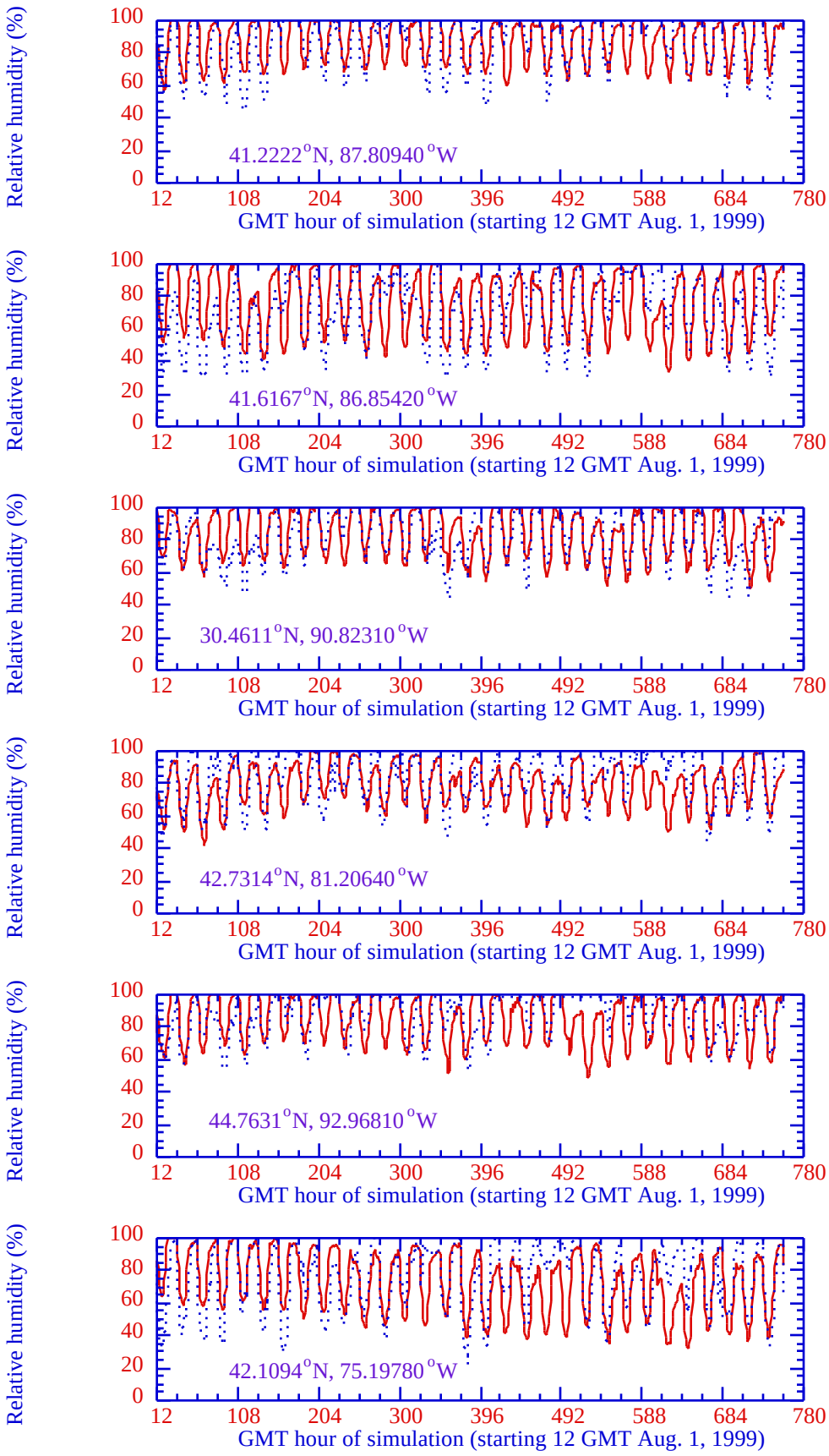
Relative humidity (%)
100
80
60
40
20
0
41.2222°N, 87.80940°W
12
108
204
300
396
492
588
684
780
GMT hour of simulation (starting 12 GMT Aug. 1, 1999)
Relative humidity (%)
41.6167°N, 86.85420°W
GMT hour of simulation (starting 12 GMT Aug. 1, 1999)
Relative humidity (%)
30.4611°N, 90.82310°W
GMT hour of simulation (starting 12 GMT Aug. 1, 1999)
Relative humidity (%)
42.7314°N, 81.20640°W
GMT hour of simulation (starting 12 GMT Aug. 1, 1999)
Relative humidity (%)
44.7631°N, 92.96810°W
GMT hour of simulation (starting 12 GMT Aug. 1, 1999)
Relative humidity (%)
42.1094°N, 75.19780°W
GMT hour of simulation (starting 12 GMT Aug. 1, 1999)

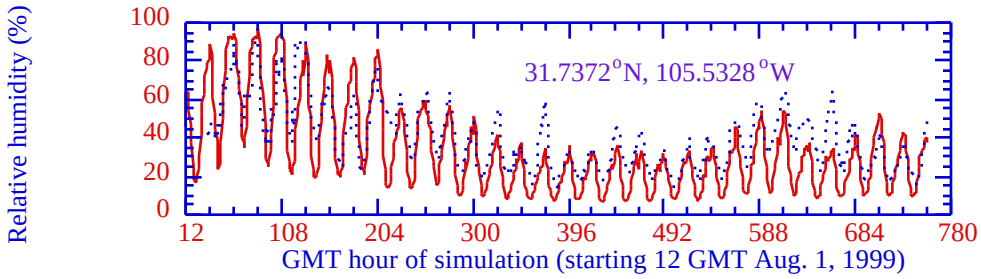

Figure 6. Comparison of August 1999 hourly modeled (solid lines) with measured (dashed lines) downward surface solar radiation [*USEPA*, 2003a] at several air quality monitoring stations in the U.S. (Only 10 days are show so that the daily variation can be seen better). See caption to Figure 1 for resolution of simulation.

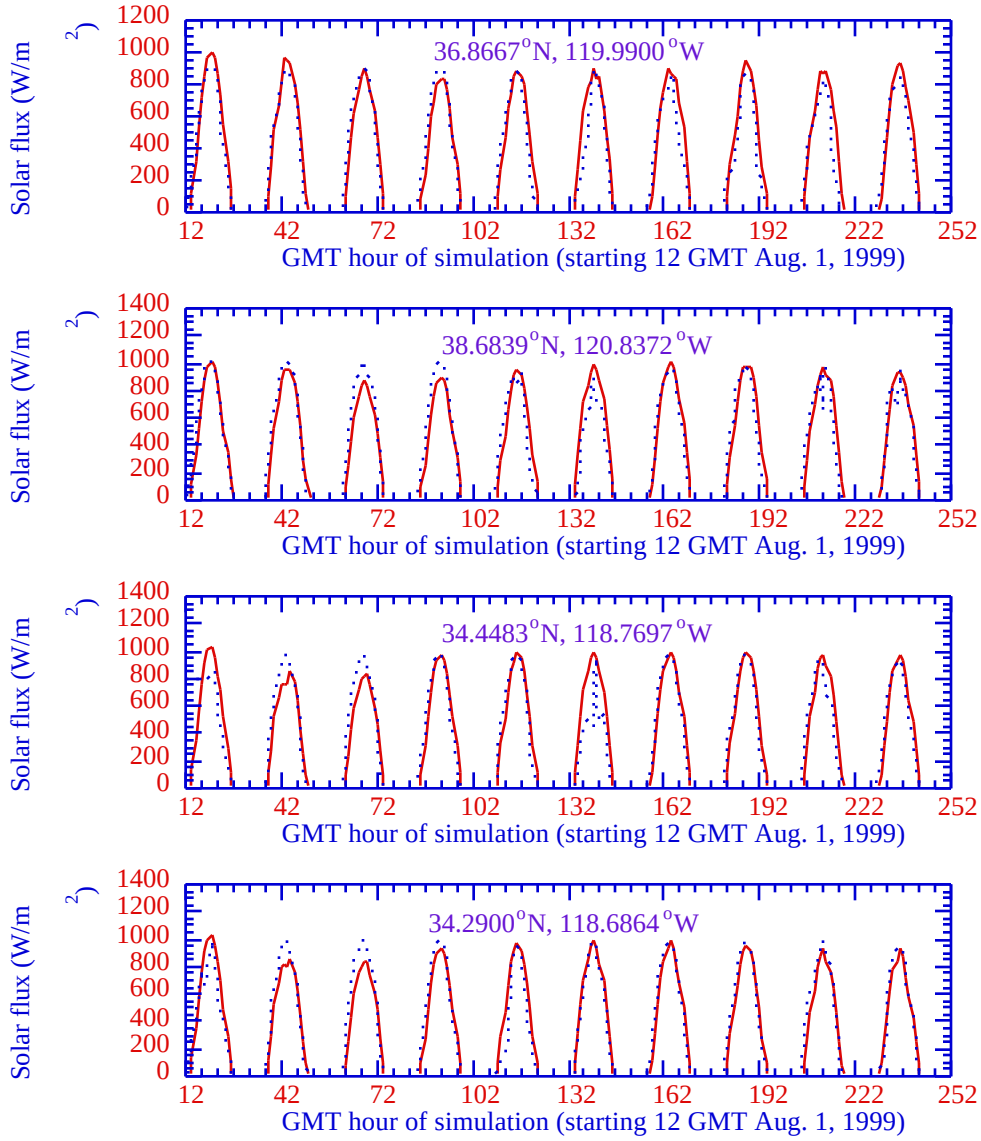

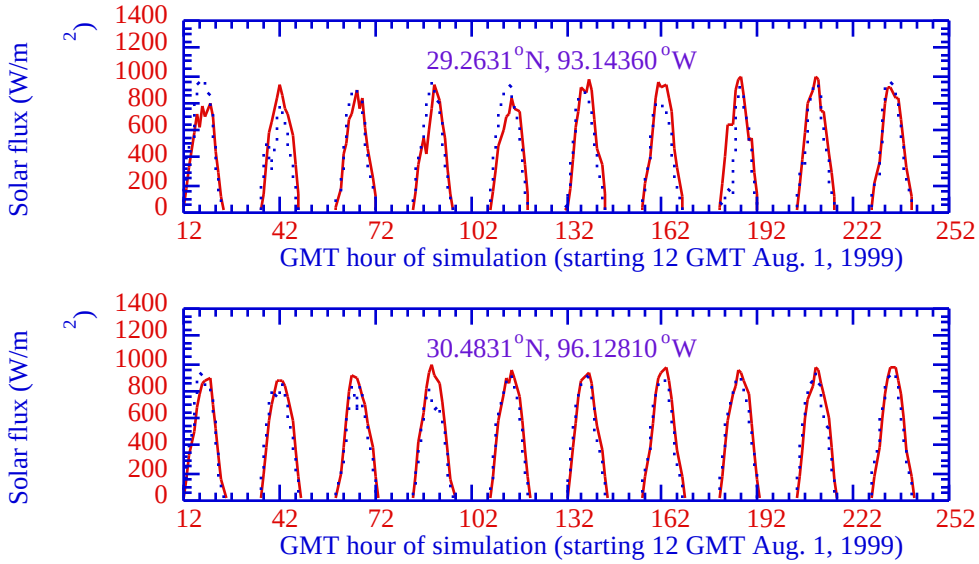

Figure 7. Comparison of August 1999 hourly modeled (solid lines) with measured (dashed lines) downward surface ultraviolet radiation [*USEPA*, 2003a] at several air quality monitoring stations in the U.S. (Only 10 days are show so that the daily variation can be seen better). See caption to Figure 1 for resolution of simulation.

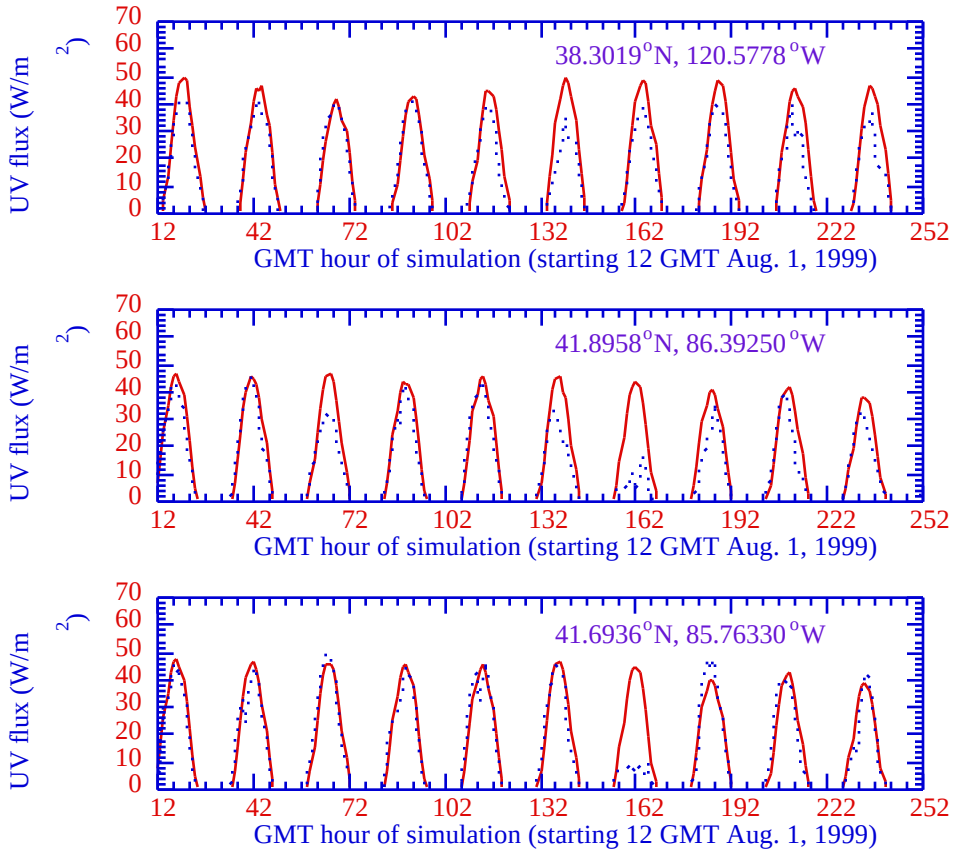

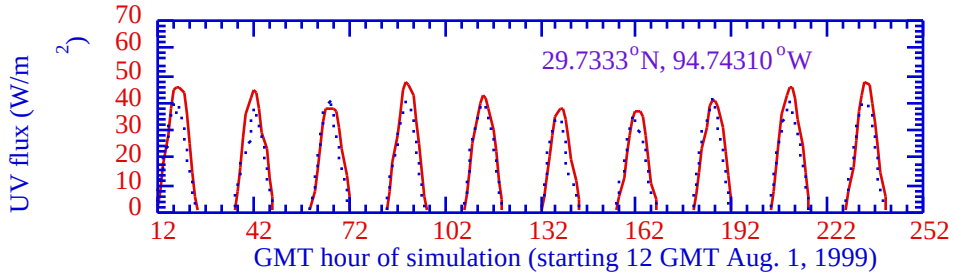

Figure 8. Comparison of August 1999 hourly modeled (solid lines) with measured (dashed lines) near-surface air temperature [*USEPA*, 2003a] at several air quality monitoring stations in the U.S. The simulations were run without data assimilation or spinup.

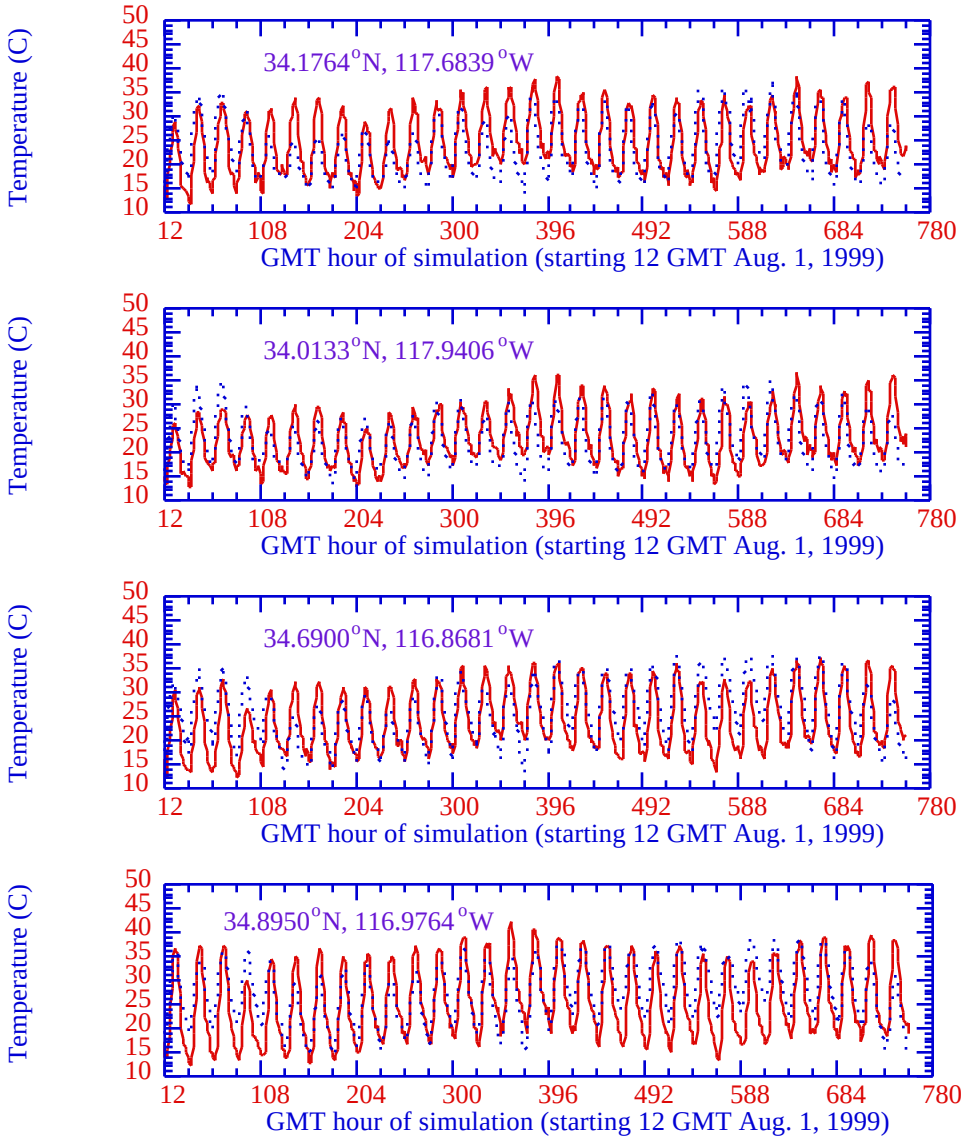

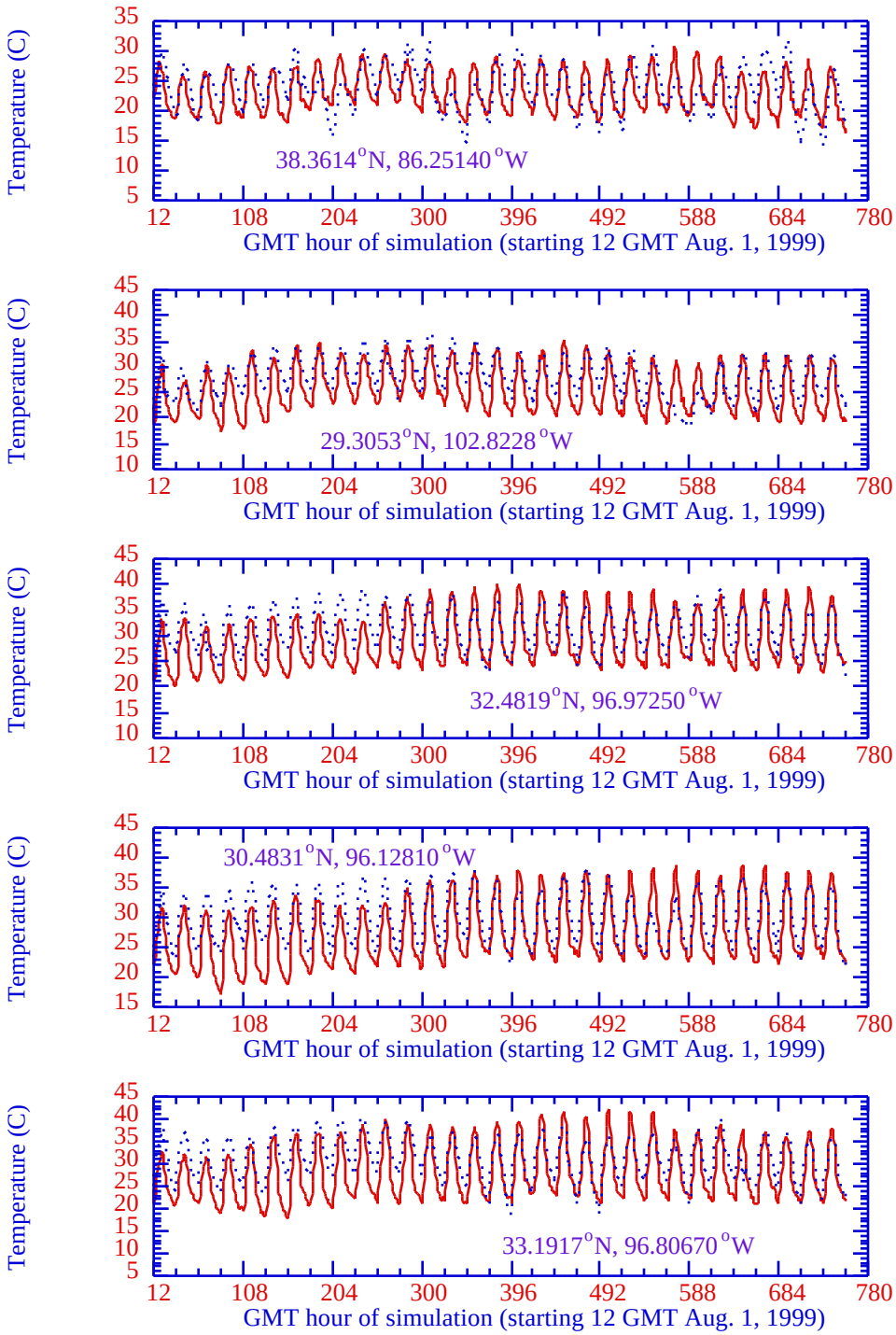

Figure 9 shows the August-average U.S. difference in NO_2, PAN, and HNO_3 following conversion to diesel in case 2. These difference plots are described in the main text, Section 2.

Figure 9. Modeled August 1999 differences (averaged over every hour in August) in (a) near-surface NO_2, (b) near-surface PAN, and (c) near-surface HNO_3 due to the U.S. conversion from gasoline to diesel

vehicles with 50% lower CO and primary HC emissions, 50% higher NO_x emissions, and an NO_2:NO ratio of 20:80 instead of 10:90 for diesel (case 2).

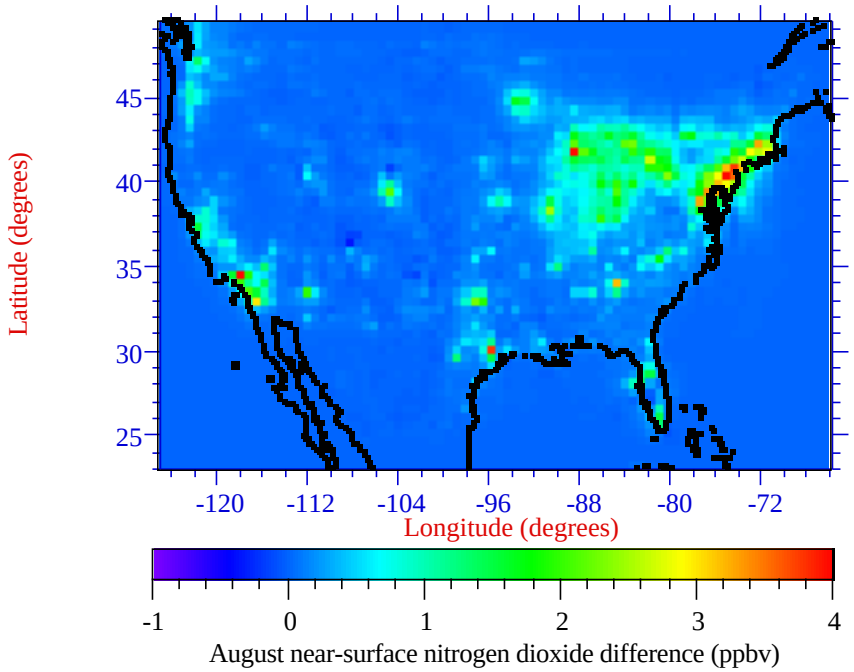

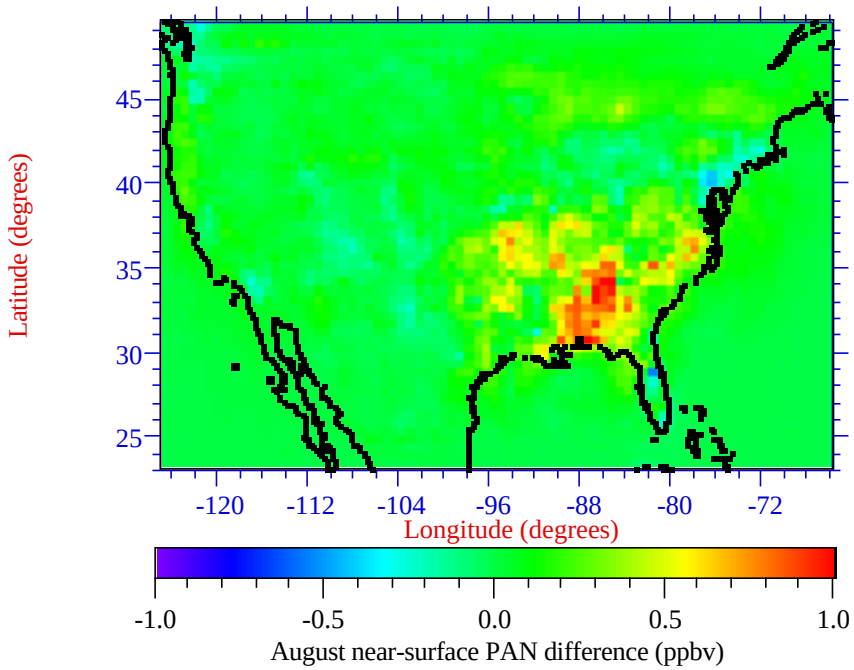

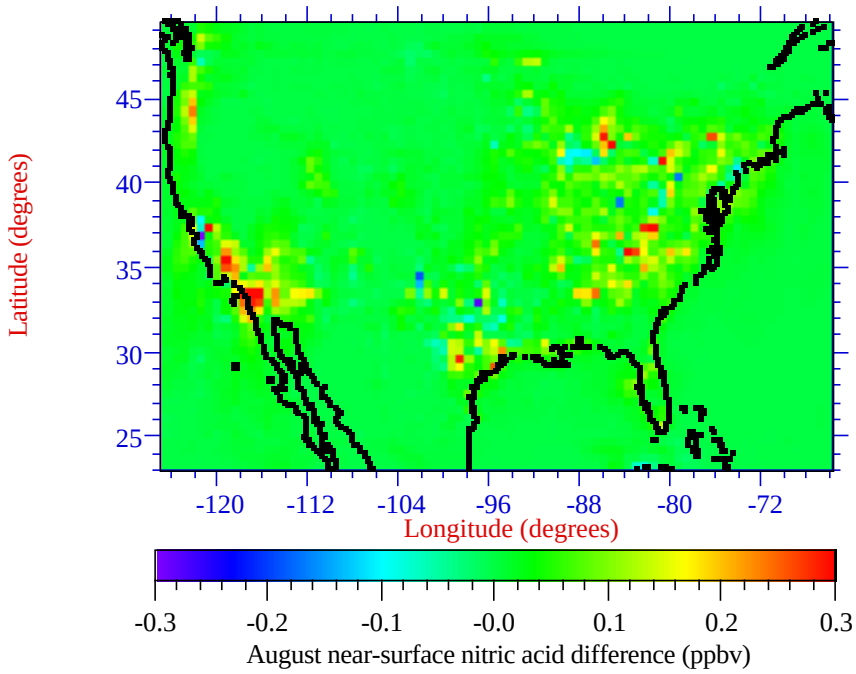

3. Brief discussion of relative effects of diesel versus gasoline on climate.
The main argument for expanding the use of diesel vehicles is that they ostensibly emit less CO_2 per distance traveled, thereby reducing the climate impact of the vehicle fleet. A counterargument is that the warming effect of BC+OM emitted by diesel vehicles without a trap in excess of that emitted by gasoline may more than offset the cooling due to reducing CO_2 for a specific period [*Jacobson*, 2002a, Section 7]. Adding a trap to diesel vehicles reduces the particle emissions by >90% (and up to 99%) (e.g., Table 1, main text) and reduces the BC content of soot particles [e.g., *Durbin and Norbeck*, 2002]. On the other hand, particle emissions from diesel vehicles with a trap may still slightly exceed those from gasoline vehicles (Table 1, main text). In addition, the trap and NO_x device increase diesel fuel use by 3.5-8.5% [*Salvat et al*., 2000; *Johnson*, 2001; *Ullman et al*., 2002; *Durbin and Norbeck*, 2002] reducing the CO_2 difference. If, after these factors are taken into consideration, the net climate advantage of gasoline versus diesel with a trap still holds, the time period of the advantage may be relatively short (e.g., on the order of a decade or so) and the magnitude of the temperature advantage during the period, small.

As such, the relative benefit of diesel vehicles with a trap versus gasoline vehicles in the long run (e.g., on the order of many decades) depends substantially on the relative CO_2 emissions, and the relative CO_2 emissions depends on which vehicles are compared. Some argue that only cars of the same engine size should be compared. Others argue that the comparison should be done based on equivalent air pollution emissions (e.g., NO_x, organics, CO, particles), since pollution affects years of life lost and mortality. This argument is supported by the present paper. A third comparison is vehicle availability. Table 1 shows the highest-mileage vehicles available in the U.S. and their corresponding CO_2 emissions. The table shows that the four-lowest CO_2 emitters are gas-electric hybrids followed by two gasoline vehicles followed by diesel vehicles. The table suggests that, for the greatest CO_2 reduction in the U.S. as of 2003, the highest-mileage gas-electric hybrid and gasoline vehicles have an advantage over the highest-mileage diesel vehicles.

Table 1. Highest-mileage passenger vehicles available in the U.S. in 2003, ranked by their CO_2 emissions (with and without a trap+NO_x filter in the case of diesel).

Vehicle	Energy source	Avg. mpg	CO_2 (g-C/km)	CO_2 (g-C/km) w/trap+filter
Honda Insight (M)	Gas/electric	64.5	23.0	
Honda Insight (A)	Gas/electric	56.5	26.2	
Toyota Prius (A)	Gas/electric	48.5	30.6	
Honda Civic (M)	Gas/electric	48.5	30.6	
Honda Civic (M)	Gas	40	37.1	
Toyota Echo (M)	Gas	39	38.0	
VW Golf, Jetta (M)	Diesel	45.5	37.8	39.7
VW Golf, Jetta (A)	Diesel	39.5	43.5	45.7

(A) denotes automatic transmission; (M) denotes manual transmission. The table assumes a gasoline and diesel density of 737 g/L and 840 g/L, respectively, a gasoline and diesel carbon content of 85.5% and 87.0%, respectively, and an increase in fuel use with a trap+filter of 5% (see text). Source of fuel economy: *DOE* [2003].

Finally, the actual difference in CO_2 also depends on what choices consumers actually make. For example, experience in Europe shows that people tend to buy larger diesel cars and drive them further than gasoline cars, obviating any potential CO_2 benefit that might have occurred in Europe over the last several years [*Schipper et al*., 2002].

In sum, there appears to be no clearcut advantage of diesel vehicles with a particle trap or gasoline vehicles on climate. With respect to air pollution in the U.S., though, this study suggests that the relative advantage of gasoline versus diesel appears to depend more on NO_x emissions than on hydrocarbon emissions. Vehicles emitting greater NO_x in the U.S. will generally enhance photochemical smog to a greater degree.

References

Association of European Automobile Manufacturers (ACEA), Programme on emissions of fine particles from passenger cars, ACEA Report, Brussels, June (2002).

Bond, T.C., Streets, D.G., Yarber, K.F., Nelson, S.M., Woo, J.-H. & Klimont, Z., *J. Geophys. Res*., submitted (2003).

Department of Energy (DOE), 2003 Fuel Economy Guide, 2003; see www.fueleconomy.gov.

Durbin, T., and J. M. Norbeck, Comparison of emissions for medium-duty diesel trucks operated on California in-use diesel, ARCO's EC-diesel, and ARCO EC-diesel with a diesel particulate filter, Final Report to National Renewable Energy Laboratory Under Contract #ACL-1-30110-01 and the Ford Motor Company, July, 2002.

Jacobson, M.Z., Lu, R., Turco, R.P. & Toon, O.B. Development and application of a new air pollution modeling system. Part I: Gas-phase simulations. *Atmos. Environ*., **30B**, 1939-1963 (1996).

Jacobson, M.Z. Development and application of a new air pollution modeling system. Part III: Aerosol-phase simulations. *Atmos. Environ*., **31A**, 587-608 (1997).

Jacobson, M.Z. GATOR-GCMM: 2. A study of day- and nighttime ozone layers aloft, ozone in national parks, and weather during the SARMAP field campaign. *J. Geophys. Res*., **106**, 5403-5420 (2001a).

Jacobson, M.Z. Global direct radiative forcing due to multicomponent anthropogenic and natural aerosols. *J. Geophys. Res*., **106**, 1551-1568 (2001b).

Jacobson, M.Z. Control of fossil-fuel particulate black carbon plus organic matter, possibly the most effective method of slowing global warming. *J. Geophys. Res*., **107** (D19) 4410, doi:10.1029/2001JD001376 (2002a).

Jacobson, M.Z. Analysis of aerosol interactions with numerical techniques for solving coagulation, nucleation, condensation, dissolution, and reversible chemistry among multiple size distributions. *J. Geophys. Res*., **107** (D19), 4366, doi:10.1029/ 2001JD002044 (2002b)

Jacobson, M.Z. Development of mixed-phase clouds from multiple aerosol size distributions and the effect of the clouds on aerosol removal. *J. Geophys. Res*., **108** (D8), doi:10.1029/2002JD002691 (2003).

Johnson, T., Developing trends – Diesel emission control update, 2001, see www.osti.gov/hvt/deer2001/johnson.pdf.

National Center for Environmental Prediction. 2.5 degree global final analyses, distributed by the Data Support Section, National Center for Atmospheric Research (2003).

Salvat, O., Marez, P. & Belot, G. Passenger car serial application of a particulate filter system on a common rail direct injection diesel engine, SAE 2000-01-0473 (2000).

Schipper, L., Marie-Lilliu, C. & Fulton, L. Diesels in Europe: Analysis of characteristics, usage patterns, energy savings and CO_2 emission implications. *J. Transport Economics and Policy*, **36**, 305-340 (2002).

Ullman, T. L., Smith, L.R. & Anthony, J.W. Exhaust emissions from school buses in compressed natural gas, low emitting diesel, and conventional diesel engine configurations, Southwest Research Institute Report 08.05303 (2002).

United States Environmental Protection Agency (USEPA). AIR Data, http://www.epa.gov/air/data/ (2003a).

United States Environmental Protection Agency (USEPA). Clearinghouse for Inventories and Emission Factors, http://www.epa.gov/ttn/chief/ (2003b).

United States Environmental Protection Agency (USEPA). Improvements in Vegetation Cover Data, http://www.epa.gov/AMD/beld3.html (2003c).

United States Geological Survey (USGS) / U. Nebraska, Lincoln / European Commission's Joint Research Center. 1-km resolution global landcover characteristics data base, derived from Advanced Very High Resolution Radiometer (AVHRR) data from the period April 1992 to March 1993 (1999).